SOILS AND FOUNDATIONS Vol. 46, No. 1, 1–14, Feb. 2006
Japanese Geotechnical Society

APPLICABILITY OF THE SMALL DIAMETER SAMPLER FOR NIIGATA SAND DEPOSITS

TAKAHARU SHOGAKI[i], RYO SAKAMOTO[ii], YOSHIHITO NAKANO[iii] and AZUMA SHIBATA[iii]

ABSTRACT

Applicability of tube sampling for Niigata sand deposits is discussed through bender element and cyclic triaxial tests for samples obtained from two-chambered hydraulic piston samplers (Shogaki, 1997) with inner diameters of 48 mm and 50 mm, a one-chambered 70 mm diameter sampler, a 125-mm rotary triple-tube sampler and the frozen (FS) sampling method (Yoshimi et al., 1989). The relationship between the relative density (D_r) and normalized SPT N-value (N_1) obtained from small diameter samplers with inner diameters of 45 mm and 50 mm samplers was close to that of the FS and the N_1 coefficient was greater than those of the 70-mm and other tube samplers. The stress ratio at 20 cycles (R_{L20}) and the initial modulus of rigidity (G_{CTX}) of samples obtained from the 45-mm and 50-mm samplers were greater than those of the 70-mm, 125-mm rotary triple-tube and other tube samplers. However, the R_{L20} values obtained from the 45-mm and 50-mm samplers were smaller than those of the FS sampler in the area of $N_1 > 24$. The G_{BE} and G_{CTX} values obtained from the 45-mm and 50-mm samplers were close to those of the FS sampling. Therefore, the 45-mm and 50-mm samplers can take equally high quality samples for Niigata sand deposits.

Key words: CPT, frozen sample, liquefaction strength, modulus of initial rigidity, relative density, sample disturbance, sand, secondary wave velocity, small diameter sampler, SPT, undisturbed tube sampling (**IGC**: C5/C6/D7)

INTRODUCTION

Studies of dynamic strength and deformation properties for geotechnical materials have been conducted since the Niigata earthquake in 1964 and the basis for design code specifications, site investigations and laboratory tests are established from those results. However, the liquefactions of soils, excluding sand, in the Hanshin Awaji earthquake of 1995 and the increasing liquefaction of various soils have made revisions of these codes necessary. These areas of research have become more important as stronger earthquakes reoccur throughout Japan, particularly the possibility of occurrence in the Kanto and Tokai regions.

The frozen sample (FS) method is useful for undisturbed clean sand in dynamic strength and deformation tests. However, it is very expensive and requires considerable equipment. It is therefore limited to geotechnical investigation of important soils, building structures and research sampling, etc. A simpler and more economical sampling method is required. In order to establish a tube sampling (TS) method for natural sand deposits and an evaluation technique for the sample quality obtained, systematic samplings were conducted by the soil sampling committee of the Japanese Geotechnical Society (JGS) in 1987 and 1988 and the Japan Geotechnical Consultant Association (JGCA) in 1998. The TS method is effective for sandy and clayey soil, but it is used predominantly for clean sand. In the JGS-1987 investigation, it was reported that there was only a 67% success rate in sampling, using this method.

Shogaki (1997) developed a new sampler called a 45-mm sampler, which has a 45 mm inner diameter with a two-chambered hydraulic piston, and its applicability was tested through unconfined compression tests at six different sites in Japan (Shogaki and Sakamoto, 2004). It was confirmed from Shogaki and Sakamoto (2004) that for Japanese clay deposits having unconfined compressive strength (q_u) ranging from 23 kPa to 604 kPa, the q_u and the secant of modulus (E_{50}) for samples obtained from this sampler were between (20～70)% and (30～90)% greater than those of the 75 mm samplers normally used in Japan, one being a non-rotary, thin-walled, single tube type with a fixed piston and the other a rotary, double-tube sampler. However, the applicability of the 45-mm sampler for sandy soil has not been confirmed.

In order to discuss the applicability of the 45-mm sampler for Niigata sand, the samples were taken by the 45-mm, 50-mm and 70-mm samplers (Shogaki et al.,

[i] Associate Professor, National Defense Academy, 1-10-20 Hashirimizu, Yokosuka 239-8686, Japan (shogaki@nda.ac.jp).
[ii] Graduate Student, ditto.
[iii] Geotechnical Engineer, Kowa Co., LTD., 6-1 Shinkou-cho, Niigata 950-8565, Japan.
The manuscript for this paper was received for review on June 25, 2004; approved on November 10, 2005.
Written discussions on this paper should be submitted before September 1, 2006 to the Japanese Geotechnical Society, 4-38-2, Sengoku, Bunkyo-ku, Tokyo 112-0011, Japan. Upon request the closing date may be extended one month.

2002). The sample recovery ratio (R_r), (which is defined in an equation as the ratio of the length of the sample before withdrawal over the penetration depth during sampling) values from the 45-mm and 50-mm samplers were greater than those of the 70-mm sampler and independent of the sands having $N=3\sim54$ from SPT (Shogaki et al., 2002).

In this paper, applicability of the small diameter sampler for Niigata sand deposits obtained from Shogaki et al. (2002) is discussed through the bender element (BE) and cyclic triaxial (CTX) tests for samples obtained from two-chambered hydraulic piston samplers (Shogaki, 1997), with inner diameters of 48 mm and 50 mm, a one-chambered sampler having a 70 mm diameter, a 125-mm rotary triple-tube sampler and FS (Yoshimi et al., 1989).

SAMPLING SITE, SAND SAMPLING AND IN-SITU TESTING

The undisturbed sand sampling, using the 45-mm, 50-mm and 70-mm samplers, was conducted in 2002 at the Meike elementary school in Niigata city (2000 investigation). The sampling site sediment was medium sand, in which 50% of the grain size is about 0.25 mm and the percentage of grain size smaller than 0.075 mm (F_c) is about 1%. Undisturbed tube sampling in this sand is generally very difficult. Yoshimi et al. (1989) took sand samples using the FS and the 125-mm rotary triple-tube sampler at the same site in 1986 (1986 investigation) and the soil sampling committee of the Japanese Society for Soil Mechanics and Geotechnical Engineering also conducted systematic sampling at the same site using various types of tube samplers (1987 investigation) in order to establish a tube sampling method for natural sand deposits and an evaluation technique for the sample quality obtained (Japanese Geotechnical Society, 1988).

Figure 1 shows the layout of the geotechnical investigation site, including the 1986/1987 investigation areas. This paper's authors did the tube sampling, SPT and CPT in the 2000 investigation area on the eastern side of the 1986/1987 investigation areas. Table 1 shows the abbreviation for the sampling method/sampler used in the 1986/1987 investigations and its tube inside diameter. Also the specifications for samplers used in the 2000 investigation are summarized in Table 2. The 70-mm sampler has the same mechanical apparatus as the 75-mm sampler (JGS 1221-2003) normally used in Japan, both having a non-rotary thin-walled, single tube with a fixed piston. However, they differ by inside diameter and thickness of tube. The samples obtained from the 2000 investigation were frozen by dry ice at the site after the pore water was drained through a cap of porous stone in a procedure similar to that of the 1987 investigation.

Figure 2 shows the sampling locations and the in-situ test results. The N, q_c values and the secondary (S) wave velocity (V_s) are plotted against the depth (z) in Fig. 2. The CPT were performed in accordance with the Japanese Geotechnical Standard for electric cone penetration test (JGS 1435-2003). Based on the N and the q_c values, it was reported by JGS (2004) that the layer at a depth of 2 m to 7 m was a sand hill and the lower sand layer at a depth greater than 7 m had been deposited by river water. The test results were classified by tested year. The q_c values obtained from the 1987 and 2000 investigations are almost similar and there is no stress change caused by soil alteration. Therefore, it can be judged that the geotechnical properties at equal depths throughout this area are almost similar. The N values obtained from

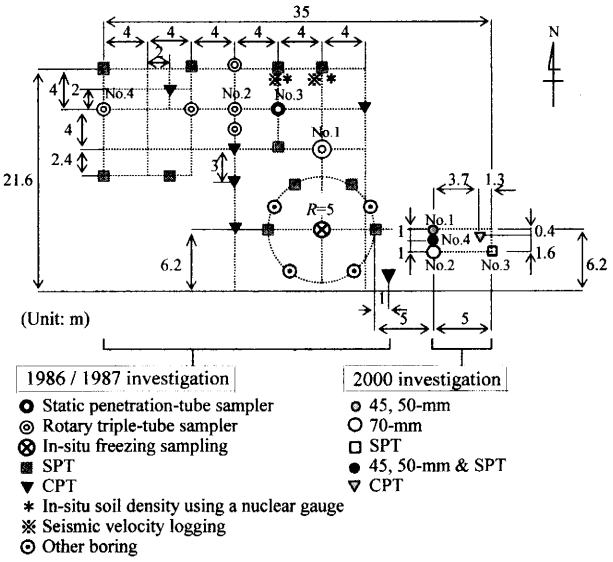

Fig. 1. Layout of the geotechnical investigation sites

Table 1. Specifications of samplers used in the 1986 and 1987 investigations

Bore.	Sampling method or sampler	Abbreviation	D_i
1	125-mm rotary triple-tube sampler	125T	125
3	Static penetration-tube sampler	50SP, 70SP	50, 70
4	Triple-tube sampler (pressure control type)	81T(P)	81
2	81-mm rotary triple-tube sampler	81T	81
5	83-mm rotary triple-tube sampler	83T	83
—	In-situ freezing sampling	FS	—

D_i: Inside diameter of tube (mm)

the 2000 investigation are slightly greater than those of other investigations. The trip tonbi and monkey methods for measuring the N value were used in the 1986/1987 and 2000 investigations, respectively. It is well known that the accuracy of the measured N value is controlled by the striking efficiency of the hammer. Seed et al. (1983) measured the striking efficiency of the monkey and tonbi methods and showed the conversion equation of them as Eq. (1).

$$N_{65} = 1.2N_{78} \tag{1}$$

where, N_{65} and N_{78} are N values obtained from monkey and tonbi, respectively.

The converted N values (□) from Eq. (1) (solid and broken lines) are close to those of the 1986 investigation. The mean N values (○) obtained from the 1986 and 1987 investigations, as shown in Fig. 2, are used for a discussion concerning dynamic strength properties, since the undisturbed sand samples obtained from various types of samplers are located throughout the investigation site, as shown in Fig. 1. The V_s values show the test results of the 1987 investigation and these values were obtained from downhole and crosshole methods. The latter method can measure depth continuously.

Table 2. Specifications of samplers used in the 2000 investigation

Sampler	45-mm	50-mm	70-mm
Length of sampler (mm)	1340	1680	1165
Weight of sampler (kg)	10.6	12.8	21.4
Greatest outside diameter of sampler (mm)	60	60	90
Length of tube (mm)	600	800	950
Greatest outside diameter of tube, D_2 (mm)	52	56	76
Inside diameter of tube, D_1 (mm)	48	50	70
Thickness of tube (mm)	2	3	3
Edge taper angle (°)	5.4	6.6	31.0
Thickness of edge (mm)	0.2	0.2	0.2
Inside clearance (mm)	0	0	0
Area ratio, C_a (%)	17	25	18
Maximum sample length (mm)	535	735	796

GRAIN SIZE DISTRIBUTION PROPERTIES OF SAMPLES AND CYCLIC TRIAXIAL/BENDER ELEMENT TESTS

Figure 3 and Table 3 show the curves and results of grain size distribution tests for the samples obtained from the split barrel of SPT. The percentage of grain size smaller than 0.075 mm is about 1%, excluding (4～7)% of $z = -(8 \sim 10)$ m, and the uniformity coefficient and coefficient of curvature are about 1.5 and 1 with the medium grain size (D_{50}) being about 0.25 mm. The drilling mud is used for stabilization of the borehole wall for the TS but not the FS method. Through inspection of the sample at the sampler cutting edge and top surface, it was confirmed that there was no drilling mud intrusion of the sample. Therefore, it has no effect on the strength and deformation characteristics of specimens.

The cyclic triaxial tests for the undisturbed sands were performed according to the standards of the Japanese Geotechnical Society (JGS) for the Preparation of Soil Specimens for Triaxial Tests (JGS 0520-2000), the Method for Cyclic Undrained Triaxial Tests on Soils (JGS 0541-2000) and the Method for Cyclic Triaxial Tests to Determine Deformation Properties of Geomaterials

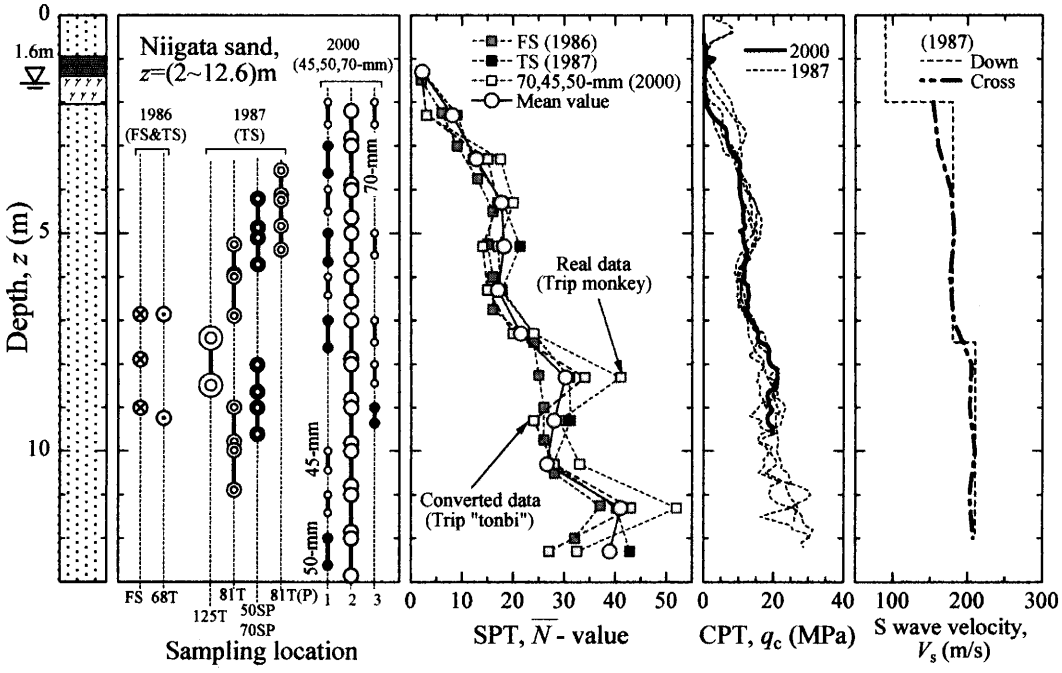

Fig. 2. Sampling location and test results of SPT, CPT and S wave velocity against the depths

(JGS 0542-2000). The procedures that are not explained in these standards are performed as follows.

Figure 4 shows the layout of the cyclic triaxial test apparatus with the bender elements at the cap and pedestal. The specimen size is 50 mm in diameter (d) and 100 mm in height (h) and the CTX apparatus can also test 50 mm and 75 mm in h specimens using the spacer shown in Fig. 4. The specimen size obtained from the 45-mm sampler is 48 mm in d and 96 mm in h since the inner diameter of the sampler is 48 mm*. The liquefaction strength and the initial modulus of rigidity (G_{CTX}) decrease with decreasing specimen diameter caused by the effect of membrane penetration. However, the medium size in Niigata sand is about 0.25 mm and is considered medium sand. The effect of membrane penetration is negligible since the exposed specimen surface can be trimmed smoothly.

The confined pressure (σ_c') for a specimen under consolidation and shear is set to the in-situ effective stress

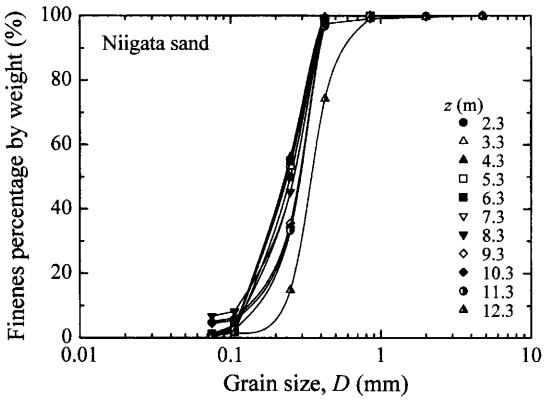

Fig. 3. Grain size distribution curves

Table 3. Results of grain size distribution tests

z (m)	D_{max} (mm)	Gravel (%)	Sand (%)	Silt & clay (%)	D_{60} (mm)	D_{50} (mm)	D_{30} (mm)	D_{10} (mm)	Uc	Uc'
1.3	4.75	8.6	75.0	16.4	0.26	0.23	0.16	—	—	—
2.3	0.85	0.0	98.9	1.1	0.27	0.25	0.21	0.15	1.8	1.0
3.3	0.85	0.0	99.1	0.9	0.26	0.24	0.20	0.14	1.9	1.0
4.3	0.85	0.0	98.9	1.1	0.26	0.24	0.20	0.14	1.8	1.1
5.3	0.85	0.0	98.8	1.2	0.26	0.24	0.20	0.14	1.9	1.1
6.3	0.85	0.0	98.9	1.1	0.26	0.24	0.20	0.15	1.8	1.1
7.3	0.85	0.0	98.7	1.3	0.28	0.26	0.22	0.16	1.7	1.1
8.3	0.85	0.0	93.2	6.8	0.28	0.26	0.21	0.13	2.2	1.2
9.3	0.85	0.0	94.9	5.1	0.30	0.28	0.24	0.17	1.7	1.1
10.3	4.75	0.3	95.2	4.5	0.30	0.28	0.24	0.18	1.7	1.1
11.3	4.75	0.1	99.0	0.9	0.29	0.28	0.24	0.19	1.5	1.1
12.3	4.75	0.4	99.0	0.6	0.37	0.34	0.29	0.23	1.6	1.0

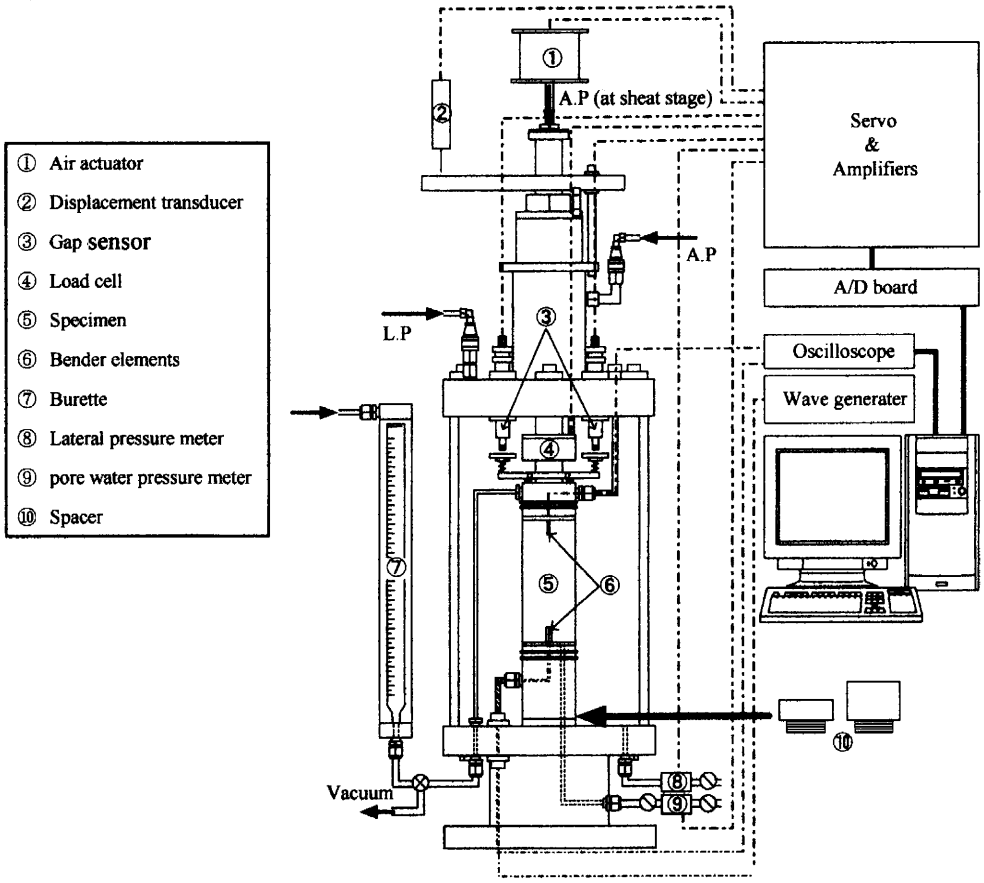

Fig. 4. Layout of the cyclic triaxial test apparatus

of the specimen. The frequency under cyclic loading is 0.1 Hz for measuring the G_{CTX} and 0.5 Hz for the liquefaction test. The cyclic loading for measuring the G_{CTX} is controlled with an axial strain less than 1×10^{-5} μm.

The specimens were trimmed from a block 12 cm in h. When the sample was withdrawn from the tube for specimen trimming, sample thawing was prevented by the use of liquified nitrogen. Specimen thawing was done under $\sigma'_c=20$ kPa after insertion in the apparatus. First, back pressure air at 200 kPa was applied to the specimens, then carbon dioxide used to remove the air and finally, the specimen was saturated with airless water, the latter two processes taking about 3 hours. Skempton's pore pressure coefficient values were greater than 0.96 for all specimens.

The testing procedures from BE to CTX are as follows;

1) The specimen was set up on the pedestal and saturated after thawing.
2) The G_{BE} of the specimen was measured by BE.
3) The G_{CTX} of the specimen was measured by CTX.
4) The liquefaction strength was measured by CTX.

The G_{BE} value was calculated by the measured V_s of the long axial direction of the specimen, as shown in Fig. 4.

The displacement of the specimen under cyclic loading, at a small strain level, was measured by the gap sensors (GS). It is known that the equivalent deformation modulus (E_{eq}) obtained from the GS method is less than that of the local displacement transducer (LDT) because of the bedding error between the cap/pedestal and specimen. Tokimatsu and Uchida (1990) and Uchida (2003) reported that the E_{eq} values of d50 mm and h100 mm specimens obtained from the frozen samples used in the GS and LDT methods were similar. The test results by JGS (Shibuya et al., 1995) of both methods on the deformation properties of Toyoura sand showed similar values for $D_r=50\%$. However, there was a difference for $D_r=80\%$. The D_r values of Niigata sand are (45~73)%. The top and bottom surface smoothness of the specimens were ensured by using a special miterbox. Therefore, the bedding error effects for G_{CTX} are not considered in this study.

THE EFFECT OF SAMPLING METHODS ON THE RELATIVE DENSITY OF NIIGATA SAND

The Effect of Sampling Tube Diameter on the Relative Density

The ratios of the relative density ($\overline{D}_{r(45,50)}$) of the specimens obtained from the 45-mm and 50-mm samplers to those of the mean value ($\overline{D}_{r(70)}$) for the specimens from the 70-mm sampler are plotted against $\overline{D}_{r(70)}$ in Fig. 5. It can be seen that the $\overline{D}_{r(45,50)}/\overline{D}_{r(70)}$ ratios decrease with increasing $\overline{D}_{r(70)}$. The possibility of increasing the sample recovery ratios (R_r) of the 70-mm samples is smaller than that of the 45-mm and 50-mm samples since the relative densities of the 70-mm samples were smaller (Shogaki et al., 2002). However, it was reported by Yoshimi (1994) that the liquefaction strength of samples under $D_r\fallingdotseq50\%$

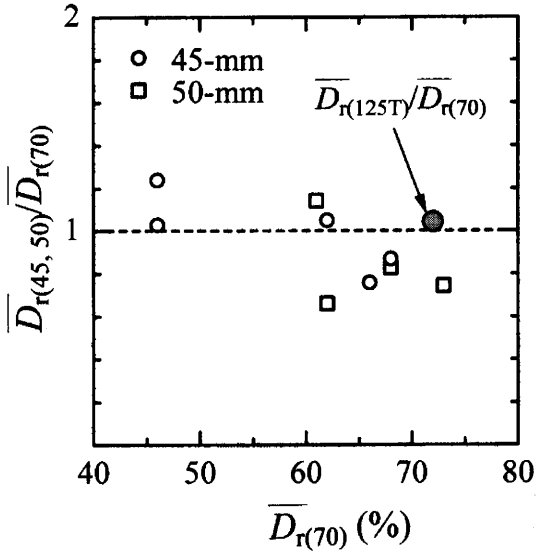

Fig. 5. Relationship between $\overline{D}_{r(45,50)}/\overline{D}_{r(70)}$ and $\overline{D}_{r(70\text{-mm})}$

obtained from the FS and TS samplers are similar. The ratios of relative density under $D_r\fallingdotseq50\%$ are almost 1 in Fig. 5. This means that the D_r of a sample under $D_r\fallingdotseq50\%$ is independent of the tube diameter used in this study and this coincides with Yoshimi (1994). Therefore, Fig. 5 shows the applicability of the small diameter sampler for Niigata sand. The $\overline{D}_{r(125T)}/\overline{D}_{r(70)}$ ratio for the samples from the triple tube sampler (125T) and obtained from the 1987 investigation is also plotted in Fig. 5. This ratio is also about 1 and the $\overline{D}_r$ values of the 125 T and 70-mm samplers are similar.

The Effect of the Sampling Method on the Relative Density

Figure 6 shows the relationship between the N and D_r values. The N values are converted to N_1 value using Eq. (2), proposed by the Japan Public Highway Corporation (Specifications for highway bridges, 2003), in order to consider the effect of the effective overburden pressure.

$$N_1=170N/(\sigma'_v+70) \tag{2}$$

The results of the FS and TS from the 1986 and 1987 investigations and Eq. (3) by Meyerhof (1956) are converted to N_1 and also shown in Fig. 6.

$$D_r=208\sqrt{\frac{N}{\sigma'_{vo}+69}} \tag{3}$$

The straight line, mentioned as Eq. (4) in Fig. 6, is a regression line obtained from the least square method for the plots of the FS sample. The D_r value of FS increase with increasing N_1.

$$D_r=1.98N_1+13.45 \tag{4}$$

The regression lines obtained from the plots of other samplers in the range of N_1 as well as Eq. (4) are also shown in Fig. 6 and summarized in Table 4. The regression line for the 45-mm and 50-mm samplers is close to that of the FS sample and the N_1 coefficient is

Table 4. Relationships between D_r and N_1 used in Fig. 6

Sampler	Regression line (Fig. 6)		Correlation coefficient
FS	——	$D_r = 1.98N_1 + 13.45$	0.954
45-mm/50-mm	——	$D_r = 1.13N_1 + 31.86$	0.598
70-mm	·····	$D_r = -0.13N_1 + 68.96$	0.061
Other TS	----	$D_r = 0.22N_1 + 66.02$	0.145

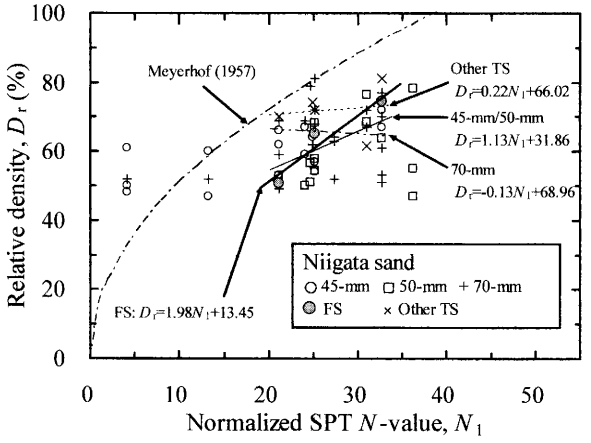

Fig. 6. Relationship between D_r and N_1

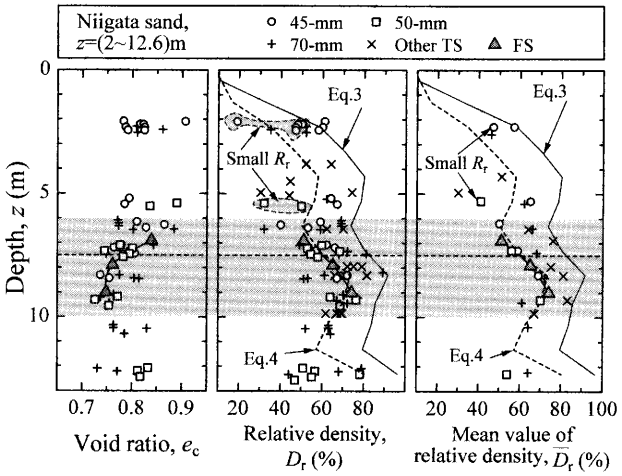

Fig. 7. The e_c, D_r and $\overline{D}_r$ values against the depths

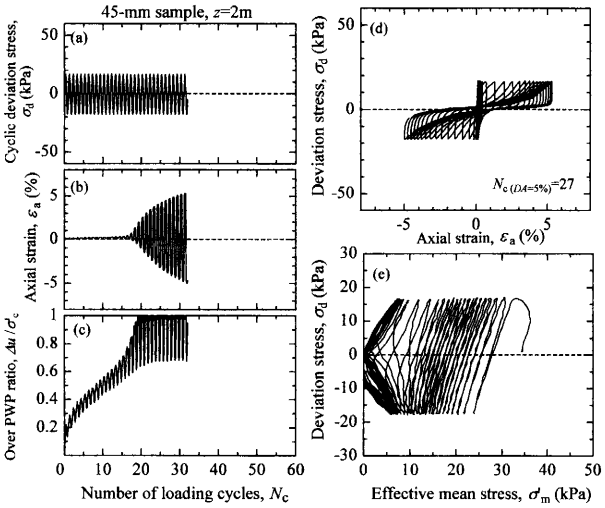

Fig. 8. Liquefaction test results (45-mm sampler, $z \fallingdotseq 2$ m)

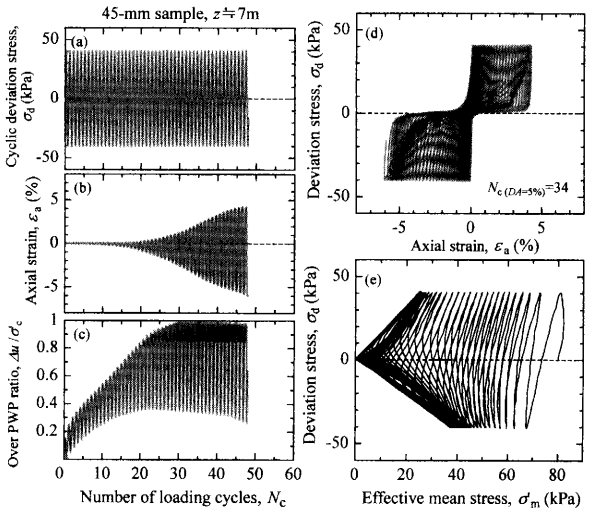

Fig. 9. Liquefaction test results (45-mm sampler, $z \fallingdotseq 7$ m)

greater than those of the 70-mm and other TS samplers. All plots, except that of $N_1 < 5$, are located at the lower part of Meyerhof's curve. This curve does not consider the effect of fine grain soil and was proposed about 50 years ago. Therefore, this curve can not describe the actual circumstances since the sampling techniques have been improved since then.

The void ratio (e_c) after consolidation of each specimen and the D_r and $\overline{D}_r$ values obtained from the TS samples, including the 45-mm and 50-mm samples, are plotted against the z in Fig. 7. The broken lines in Fig. 7 are the estimated lines of D_r and $\overline{D}_r$ obtained from Eq. (4) using the mean N value (○) as shown in Fig. 2. The D_r and $\overline{D}_r$ values obtained from Eq. (3) are also shown as straight lines in Fig. 7. This is reflected in Fig. 6, as all plots are located on the lower part of the solid line, Eq. (3) proposed by Meyerhof (1957). The $\overline{D}_r$ values in the shaded area of $z = (6 \sim 10)$ m for the TS samples are similar to those of the FS samples and very close to the estimated line in Eq. (4). Therefore, it can be assumed that the density change from the in-situ condition is small. However, the plots obtained from the 70-mm sample and the TS sample from the 1987 investigation are located at the upper part of the broken line in Eq. (4). The sample density increased with tube penetration. The plots, in which the R_r values are small and caused by sample disturbance through loss of sample near the cutting edges of the tube, are indicated as "small R_r". It is mentioned in JGS (2004) that the R_r value is an index of sample disturbance. The smaller D_r values in these plots were located close to the tube cutting edge, therefore the void ratios of these specimens increased with loss

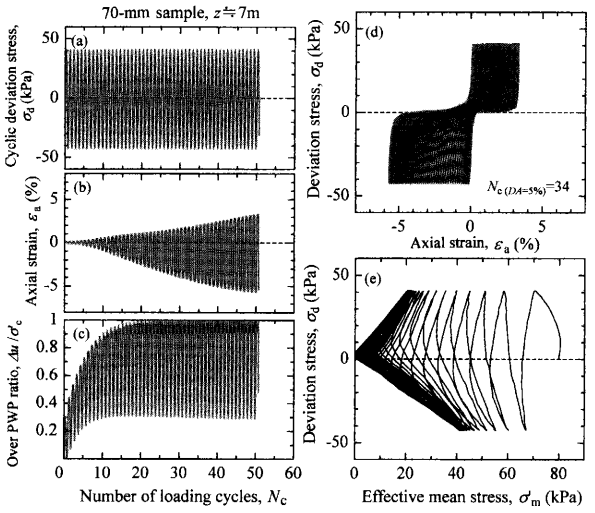

Fig. 10. Liquefaction test results (70-mm sampler, $z \fallingdotseq 7$ m)

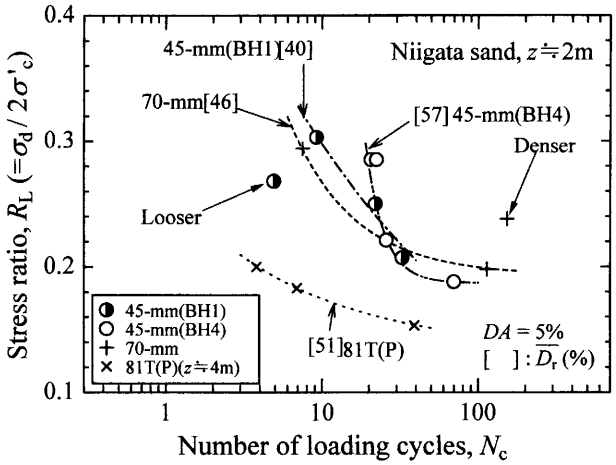

Fig. 11. Relationship between R_L and N_c ($z \fallingdotseq 2$ m)

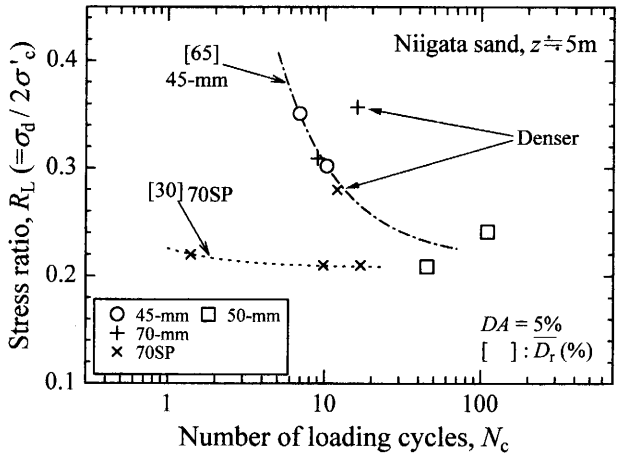

Fig. 12. Relationship between R_L and N_c ($z \fallingdotseq 5$ m)

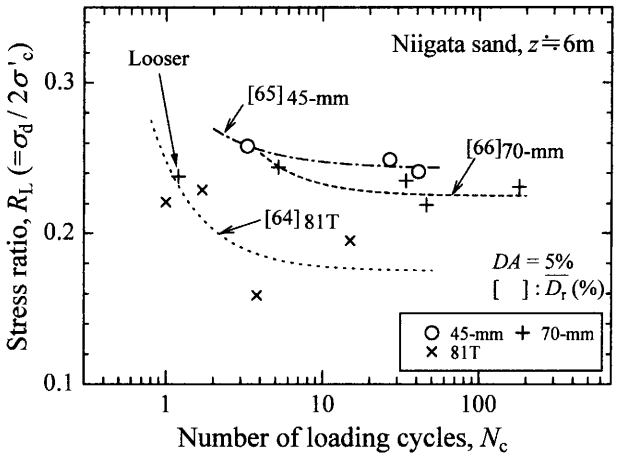

Fig. 13. Relationship between R_L and N_c ($z \fallingdotseq 6$ m)

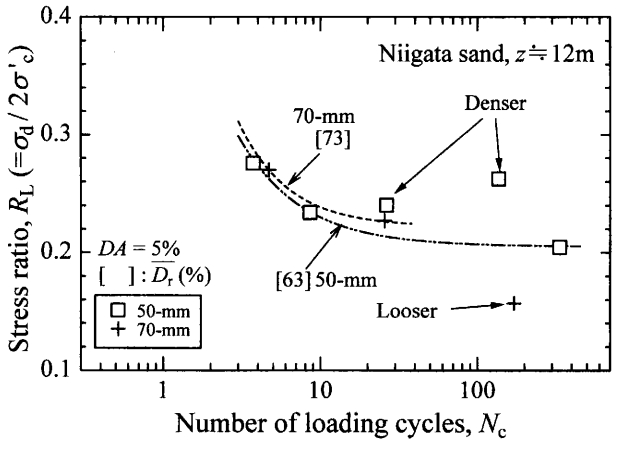

Fig. 14. Relationship between R_L and N_c ($z \fallingdotseq 12$ m)

of sample near the cutting edges of the tube. However, for a specimen obtained from the same tube, the plots further up in the sampling tube are located close to the estimated line by Eq. (4) for the 50-mm sample at $z \fallingdotseq 5.5$ m. The D_r value for the samples obtained from the 45-mm sampler of $z \fallingdotseq 2$ m are located between Eqs. (3) and (4). This means that the decreasing D_r values caused by loss of sample near the cutting edge are confined to narrow limits. The plots of the TS sample of $z < 6$ m, except in the 1987 investigation, have larger values than the estimated ones by Eq. (4). The sample density increased with tube penetration in this area. The D_r values of plots from the 50-mm and 70-mm samples at $z \fallingdotseq 12$ m are smaller than those of Eq. (4). It is well known that the sample densities obtained from the TS, for soil having large N values, decrease because of tube penetration and withdrawal. This was the situation for the sample at $z \fallingdotseq 12$ m.

The reliability of the analysis of D_r on depth is not 100% certain, since there are no test results for the FS sample and the D_r value for it is estimated from Eq. (4). However, it is shown in a later section that the above analysis is not contradictory to liquefaction test results.

Table 5(a). Test results of the bender and cyclic triaxial tests (2000 investigation)

z	N	N_1	$\bar{D}_r$ (%)	$\bar{V}_s$ (m/s)	$\bar{G}_{BE}$ (MPa)	$\bar{G}_{CTX}$ (MPa)	R_{L20}	$\bar{G}_{BE}/G_F$	$\bar{G}_{CTX}/G_F$	$\bar{e}_c$	$\overline{e_0/e_c}$	R_r (%)
(70-mm)												
2.6	8	13	46	177	59	28	0.23	1.28	0.62	0.83	1.05	94
5.4	18	24	62	180	30	37	0.24	0.98	0.61	0.79	1.01	95
6.4	17	21	66	215	86	81	0.24	1.47	1.40	0.78	1.01	83
7.4	22	25	68	184	63	51	0.25	0.93	0.76	0.79	1.01	84
8.4	30	33	72	186	49	61	0.26	0.83	0.77	0.75	1.02	92
9.4	30	31	61	229	102	95	0.28	1.24	1.16	0.79	1.04	95
10.4	28	27	64	222	94	90	0.28	1.16	1.11	0.77	1.04	95
12.4	41	36	73	216	89	66	0.23	1.09	0.81	0.75	1.01	88
(45-mm)												
2.3	8	13	57	182	63	35	0.28	1.37	0.78	0.79	1.00	85
2.3	8	13	47	171	55	54	0.25	1.20	1.19	0.82	1.00	97
5.3	18	25	65	180	60	42	0.24	0.99	0.70	0.79	1.01	96
6.2	18	24	50	191	67	70	0.25	1.16	1.21	0.83	1.01	74
7.3	17	21	59	187	64	45	0.23	0.97	0.68	0.79	1.02	94
(50-mm)												
5.3	18	25	41	159	48	64	0.23	0.81	1.07	0.86	1.01	95
7.3	22	25	56	214	86	81	0.24	1.30	1.22	0.79	1.01	96
9.3	30	31	70	229	101	96	0.26	1.27	1.21	0.75	1.07	71
12.3	41	36	54	220	92	62	0.22	1.10	0.75	0.82	1.02	89

EFFECT OF SAMPLING PROCEDURE ON LIQUEFACTION STRENGTH PROPERTIES

Liquefaction Test Results

Figure 8 shows the liquefaction test results for the sample at $z \fallingdotseq 2$ m, obtained from the 45-mm sampler. The relationship between cyclic axial deviator stress, axial strain, ratio of excess water pressure (Δu) to effective confined pressure (σ_c') and number of loading cycles (N_c) and effective stress path are shown in Figs. 8(a), (b), (c), (d) and (e) respectively. The test results for the samples obtained from the 45-mm and 70-mm samplers at $z \fallingdotseq 7$ m are also shown in Figs. 9 and 10 respectively. It can be seen from these figures that the control and accuracy, etc. for cyclic deviation stress (σ_d) under shear meets the JGS regulations. Liquefaction occurred in the sample obtained from $z \fallingdotseq 2$ m when the Δu reached σ_c' and "cyclic mobility" occurred in the sample from $z \fallingdotseq 7$ m when the Δu reached σ_c', since its density was higher.

The relationship between stress ratio ($R_L = \sigma_d'/2\sigma_c'$) and N_c on the liquefaction test for the samples obtained from the TS sample of the $z \fallingdotseq 2$, 5, 6 and 12 m are shown in Figs. 11 to 14. These test results are also summarized in Table 5. The liquefaction strength curves, in order to decide the liquefaction strength R_{L20} (R_L under $N_c = 20$) and $\bar{D}_r$ for samples from each tube, are shown in these figures and the specimen plots, in which the D_r value disagrees with that of other specimens, are noted in the comments and they were excluded from the plots for deciding the liquefaction curve. The relationships between the R_L and N_c for the samples obtained from the 45-mm, 50-mm and 70-mm samplers have similar tendencies and the D_r values are similar and unrelated to

Table 5(b). Test results of the cyclic triaxial test (1986 and 1987 investigations)

Sampler	z (m)	N	N_1	$\bar{D}_r$ (%)	$\bar{G}_{CTX}$ (MPa)	R_{L20}	$\bar{e}_c$	$\overline{e_{c0}/e_c}$	$\bar{G}_{CTX}/G_F$	R_r (%)
(1986-investigation)										
FS-1	6.9	17	21	51	57	0.24	0.84	—	0.94	
FS-2	7.9	22	25	65	73	0.32	0.76	—	0.93	100
FS-3	9.0	30	33	74	77	0.33	0.73	—	0.98	
68T-1	6.9	17	21	76	42	0.15	—	—	0.50	—
68T-2	9.3	30	31	83	65	0.20	—	—	0.77	—
(1987-investigation)										
81T(P)	4.3	13	19	51	34	0.16	0.82	1.01	0.59	78
81T-1	6.4	17	21	64	36	0.18	0.85	1.00	0.62	99
81T-2	9.9	28	31	67	48	0.20	0.76	1.08	0.58	92
125T	8.0	22	25	75	52	0.26	0.75	1.01	0.67	67
70SP	5.0	18	25	30	28	0.21	0.89	1.01	0.46	86
50SP	8.3	30	33	81	49	0.33	0.73	0.99	0.62	99

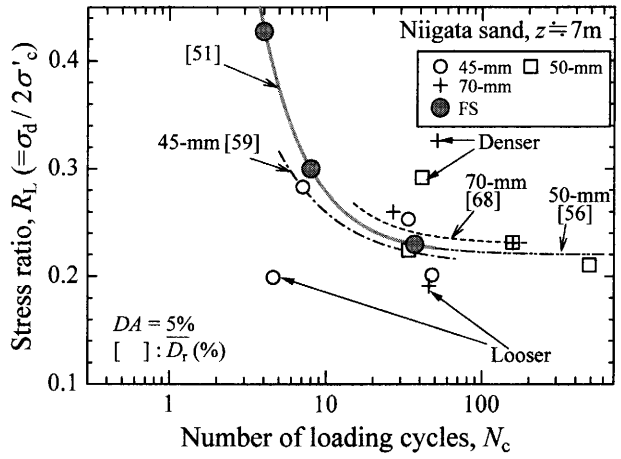

Fig. 15. Relationship between R_L and N_c ($z \fallingdotseq 7$ m)

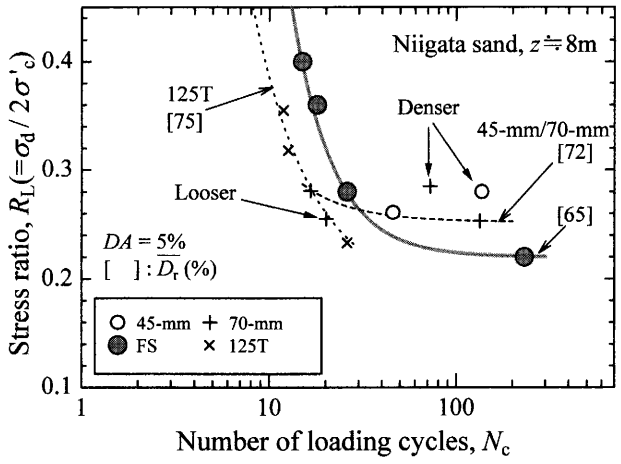

Fig. 16. Relationship between R_L and N_c ($z \fallingdotseq 8$ m)

the tube diameters. Their liquefaction strength curves have higher R_L than those of the 81T and 70SP samplers and their increase, for the $z \fallingdotseq 2$ m and 5 m samples, where the N_c value is small, is larger than that of the 1987 investigation. The reasons are as follows:

1) The borer was set-up with about a 10 tf of concrete blocks to increase the tube penetration force in the 2000 investigation. This contributed to getting a high quality sample since the tube penetration speed and force were greater than those of the 70SP, 81T and 125T in the 1987 investigation (Shogaki et al., 2002).
2) A sump for mud to avoid sand sample collapse and high mud density was used in the 2000 investigation and the R_r values were higher than those of the 1987 investigation. Therefore the sample quality was higher.
3) If the sample was disturbed in front of the cutting edge as the bit of the 81T sampler rotated. Sample disturbance is especially high for medium sand with a clay content of less than 3%.

Figure 15 shows the relationship between the R_L and N_c for the FS and TS samples obtained from $z \fallingdotseq 7$ m. The test results for $z \fallingdotseq 8$ m and 9 m are also shown in Figs. 16

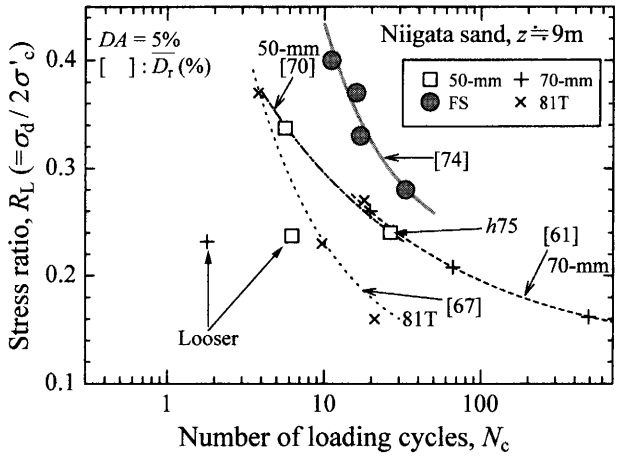

Fig. 17. Relationship between R_L and N_c ($z \fallingdotseq 9$ m)

and 17 respectively. The small variation and unique liquefaction strength curves for the plots of the FS samples indicate that these plots are mean values for several specimens and the initial stress and conditions of specimens are similar since these specimens are obtained from almost the same depths. The determination of the liquefaction strength curves for the 45-mm, 50-mm and 70-mm samplers is difficult because of the small number of plots and their scatter. However, the plots are very close to those of the FS samples. The $\overline{D_r}$ values of the 45-mm and 50-mm samplers are 8% and 5% greater than those of the FS samples respectively in Fig. 15. It was reported in the 1987 investigation (JGS, 1988) that the sample obtained from the 125T sampler is the highest quality sample of all the TS samples. The R_L values from the 125T sample increased due to increasing density since its $\overline{D_r}$ is 10% larger than those of the FS sample, as shown in Fig. 16. Due to a funding shortfall, only two boreholes were used for sampling by the 45-mm, 50-mm and 70-mm samplers, causing us to use samples from different locations inside each sampler, therefore the plot dispersions in Figs. 15 to 17 are influenced by the inherent heterogeneousness of the soils.

COMPARISON OF LIQUEFACTION STRENGTH BY LABORATORY TEST AND SITE INVESTIGATION

Many researchers have proposed estimation methods and specifications for liquefaction strength by site investigations. The sample quality obtained from the FS and TS is discussed from comparison of the liquefaction strength estimated from the site investigation and those measured values of the CTX.

Comparison between the R_{L20} Values Estimated from the N Values of SPT and Measured Ones from the CTX

There are many estimation methods for the liquefaction strength using the SPT N value and they have been used for design basis methods. On the relationship between N and R_{L20} for the conventional estimation method of the liquefaction strength in the specifications for highway bridges (2003), the Eqs. (5) and (6) are used

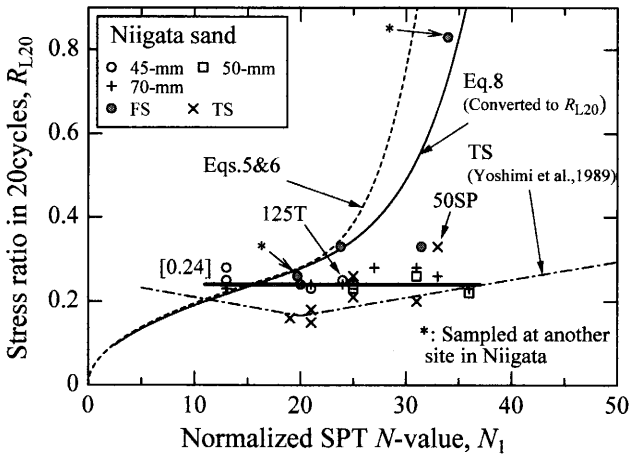

Fig. 18. Relationship between R_{L20} and N_1

for sandy soil, in which the F_c value is small.

$$R_{L20}=0.0882\sqrt{N_1/1.7} \quad (N_1<14) \tag{5}$$

$$R_{L20}=0.0882\sqrt{N_1/1.7}+1.6\times10^{-6}\times(N_1-14)^{4.5} \quad (N_1\geqq14) \tag{6}$$

Tokimatsu and Yoshimi (1983) also mentioned, for example Eq. (7), the relationship between N and R_{L15} in the case of $F_c\leqq5\%$ for the FS sample, including the concerned site.

$$R_{L15}=0.45\times\left\{\frac{16\sqrt{N_1}}{100}+\left(\frac{16\sqrt{N_1}}{97-19\log DA}\right)^{14}\right\} \tag{7}$$

where, N_1 is converted N value as shown in Eq. (2).

Figure 18 shows the relationship between N_1 and R_{L20}, obtained from Eqs. (5) and (6), and measured values. The regression lines obtained from the test results, in which Yoshimi et al. (1989) and Yoshimi (1994) carried out sampling at the concerned site and another site in Niigata city for the TS samples, are also shown in Fig. 18 by a dotted line. Yoshimi et al. (1989), Tokimatsu and Yoshimi (1983) and Yoshimi (1994) used the liquefaction strength R_{L15} (R_L under $N_c=15$) for their papers. Therefore, the R_{L15} is converted to R_{L20} using Eq. (8) by Tatsuoka et al. (1980);

$$R_L=R_{L20}(N_c/20)^{-0.1-0.1\log_{10}DA} \tag{8}$$

where, $R_{L20}\fallingdotseq1.05R_{L15}$. The R_{L20} values obtained from the design code for road bridges and Yoshimi et al. (1989) and Yoshimi (1994), preliminarily increase in the area of $N_1=15\sim22$ and exponentially increase in the area of $N_1>22$ in Fig. 18. However, the measured values differ widely from this tendency. The characteristics of measured values are summarized as follows:

1) The R_{L20} values are almost constant for the N_1 values and the mean value is 0.24.
2) The measured R_{L20} values under $N_1\fallingdotseq13$ is larger than those estimated from Eq. (7) by Tokimatsu and Yoshimi (1983) and Eqs. (5) and (6) by the specifications for highway bridges (2003).
3) The measured R_{L20} values under the same N_1 values obtained from the FS samples are greater than those of the TS samplers.
4) The R_{L20} value from 125T is almost similar to those of the 45-mm, 50-mm and 70-mm samplers, but the other TS samplers values (×) are up to a maximum of 30% smaller.

The above facts are considered as follows:

1) The R_{L20} values obtained from the 45-mm, 50-mm and 70-mm samplers are overestimated in the area of less than $N_1\fallingdotseq20$ and are caused by increased density when the sampling tube penetrates the soil and are underestimated in the area of greater N_1 values and caused by decreased density and change in grain arrangement by sample disturbance.
2) The D_r values obtained from the 45-mm, 50-mm and 70-mm samplers are similar to those of the FS in the area of $N_1=20\sim35$. However, the small change in grain arrangement caused by the shear history of tube penetration and extraction has influenced the shape of the liquefaction curve.
3) The R_r values from the 45-mm and 50-mm samples were larger than those of the 70-mm sampler and caused by the difference in tube penetration force and speed (Shogaki et al., 2002). The two-chambered hydraulic system of the 45-mm and 50-mm samplers is not the reason for the similar R_{L20} values obtained from the 125T sampler, since the R_{L20} values obtained from the 45-mm, 50-mm and 70-mm samplers are almost similar. The sampling method and the differences between rotary and static penetration samplers decide the sample quality. However, the effect of tube wall friction on sample quality is not clear since the D_r values obtained from the 45-mm and 50-mm samplers are similar to those of the FS sample and the R_{L20} values are also similar to those of the 125T sampler.

Comparison between the R_{L20} Values Estimated from the q_c of CPT and Measured Ones from the CTX

There are also many estimation methods for liquefaction strength from the CPT result. The CPT can continuously measure the soil changes at various depths. The q_c values at each 5 cm depth were measured in the 2000 investigation. Therefore, it is advantageous in a practical engineering sense that detailed liquefaction strength can be estimated from the q_c value. The estimation methods from Ishihara (1985) and Suzuki et al. (1995) are used for the comparison of the R_{L20} in this study. The method by Suzuki et al. (1995) includes the test result for the samples obtained from these authors sampling site. The q_c values obtained from each method eliminate the effect of effective overburden pressure (σ'_{vo}) from using Eqs. (9) and (10).

$$q_{t1}=[1.7/\{(\sigma'_{vo}/p_a)+0.7\}]\times q_t \tag{9}$$

$$q_{t1}=q_t/\sqrt{\sigma'_{vo}} \tag{10}$$

where, q_t is the modified tip resistance of the cone on the q_c value for water pressure and q_{t1} is the value eliminated by the σ'_{vo} from q_t. The p_a is 98.1 kPa. The q_{t1} values

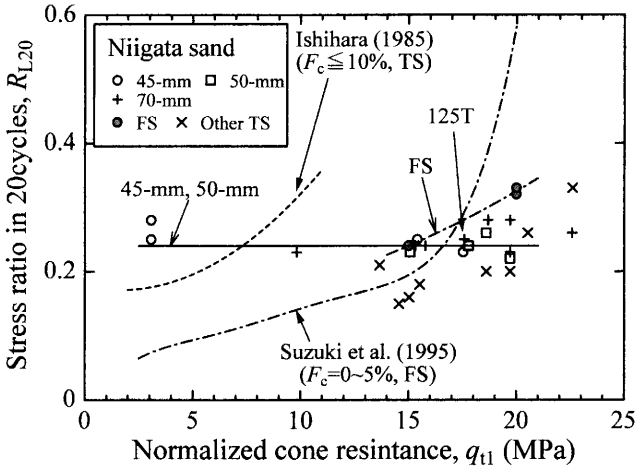

Fig. 19. Relationship between R_{L20} and q_{t1}

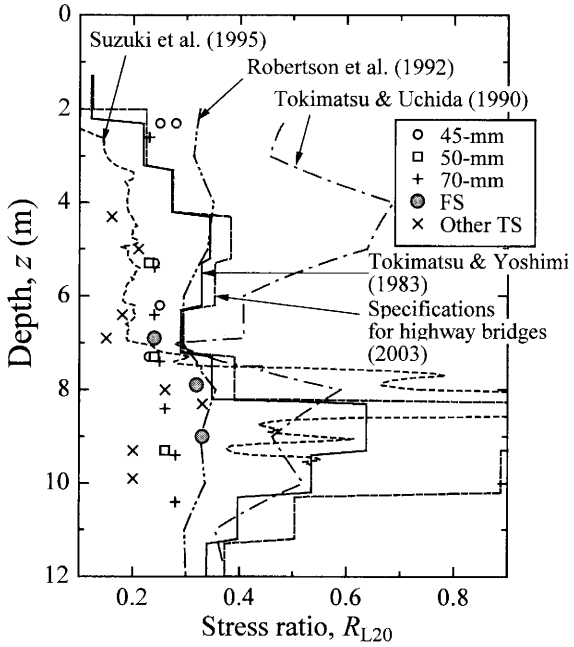

Fig. 20. The R_{L20} values against the depths

obtained from Eqs. (9) and (10) are almost similar and in the range of $\sigma'_{vo} > 30$ kPa. Therefore, in this study, Eqs. (9) and (10) are treated alike. The relationship between q_{t1} and R_{L20} are shown in Fig. 19. The regression curve by Ishihara (1985), as shown in Fig. 19, is far removed from the plots of the FS samples and the regression curve by Suzuki et al. (1995). Ishihara (1985) used the samples, $N<20$ with $F_C \leqq 10\%$, obtained from the Osterberg piston sampler, the original hydraulic piston sampler, for the regression curve. Therefore, it is thought that the R_{L20} values obtained from Ishihara's regression curve are overestimated, since the density increased with tube penetration, as described in a prior section of this paper. The R_{L20} values obtained from the FS sample and by Suzuki et al. (1995) increase with increasing q_{t1} but the measured values from the 45-mm, 50-mm and 70-mm samplers do not have those tendencies. However, the R_{L20} values obtained from the 45-mm and 50-mm samplers are similar to those of the FS sample. This reflects the liquefaction curve in Fig. 15. As per prior discussion on the N_1 value, the estimated R_{L20} values from q_{t1} for the 45-mm and 50-mm samplers are almost similar to the 70-mm and 125T samplers, but tend to be larger than the other indicated samplers.

Comparison between the R_{L20} Values Estimated from the Velocity of the Secondary Wave of the P/S Logging and Measured Ones from the CTX

Robertson et al. (1992) and Tokimatsu and Uchida (1990) are well known for their estimation methods of the liquefaction strength using the secondary wave velocity (V_s) from the P/S logging. The measurement interval of the V_s from the P/S logging is the same as that of SPT. However, the surface wave exploration method can measure the V_s not only in a vertical direction but also a horizontal one near the ground surface. Therefore, if in-situ liquefaction strength can be measured, it is advantageous from a work efficiency and economical sense of view.

The Robertson et al. (1992) method is derived from the shear stress ratio of the earthquake motion calculated from the normalized velocity of secondary wave (V_{s1}), in which the effect of σ'_{vo} is eliminated by Eq. (11).

$$V_{s1} = V_s/(\sigma'_{vo}/p_a)^{0.25} \tag{11}$$

The R_{L20} values are estimated by the figure mentioned in Robertson et al. (1992) using the V_{s1} obtained from Eq. (11) in this study. Tokimatsu and Uchida (1990) proposed the estimation method for the R_{L15} using the in-situ modulus of initial rigidity (G_F) calculated from V_s. In this study, the R_{L15} values are converted to R_{L20} from Eq. (8), after being converted to G_N from Eq. (12), using G_F values calculated from V_s of the P/S logging.

$$G_N = G/[F(e_{min})(\sigma'_m/p_a)^n]$$
$$\sigma'_m = [(1+2K_0)/3]\sigma'_{vo} \tag{12}$$

where, $F(e_{min})$ is a function of void ratio, σ'_m is the mean effective confining pressure and K_0 is the earth pressure coefficient at rest.

The in-situ R_{L20} values estimated from the methods by Tokimatsu and Yoshimi (1983), Suzuki et al. (1995), Robertson et al. (1992) and Tokimatsu and Uchida (1990) and the R_{L20} values obtained from Fig. 18 are plotted against depths in Fig. 20. The R_{L20} values obtained from TS sampling, including the 45-mm and 50-mm samplers, underestimate the in-situ value. The R_{L20} values estimated from Suzuki et al. (1995) are the smallest values in the area of $z<7$ m and they can adequately describe the measured values, except for the plots of $z \fallingdotseq 2.5$ m. However, the estimated values can not explain the measured values because the measured R_{L20} value increases in the area of $z>7.5$ m. On the other hand, the R_{L20} values obtained from Robertson et al. (1992) can adequately describe those of the FS sample in the area of $z \geqq 8$ m. The R_{L20} values obtained from the FS sample are

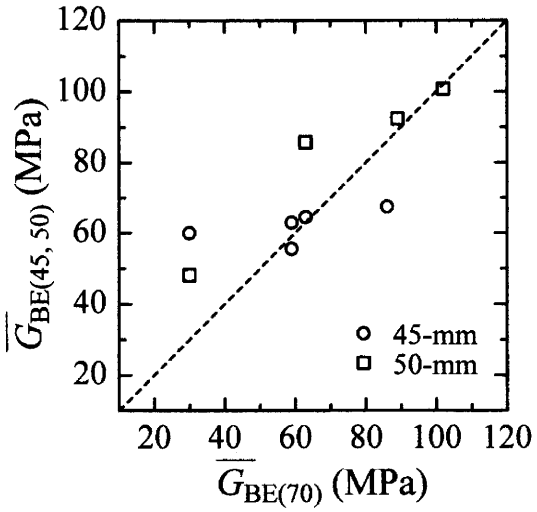

Fig. 21. Comparison of mean values of G_{BE} obtained from the 45-mm, 50-mm and 70-mm samplers

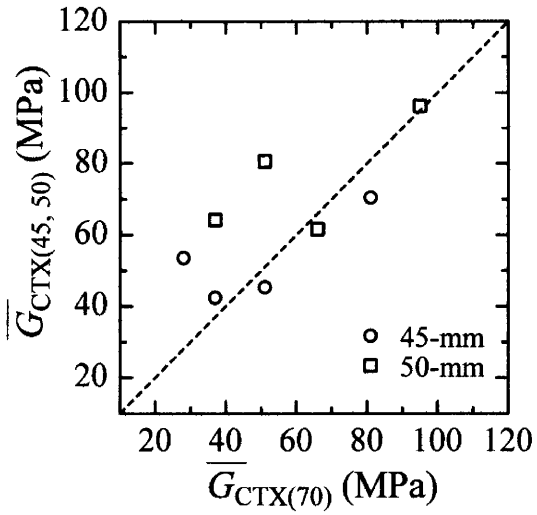

Fig. 22. Comparison of mean values of G_{CTX} obtained from the 45-mm, 50-mm and 70-mm samplers

close to those of the in-situ value.

Effect of Sampling Method Influencing the Initial Modulus of Rigidity in Niigata Sand

The sample quality obtained from the 45-mm and 50-mm samplers is evaluated from G_{BE} and G_{CTX} before the liquefaction test for each specimen. Figures 21 and 22 show the comparisons of the mean values, $\overline{G}_{BE}$ and $\overline{G}_{CTX}$ respectively, of G_{BE} and G_{CTX} and that of the 70-mm sampler. The G_{BE} and G_{CTX} values obtained from the 45-mm and 50-mm samplers are greater than those of the 70-mm sampler and the sample quality is higher. These results are corroborated in Figs. 23 to 25, as shown later.

The $\overline{D}_r$, $\overline{G}_{BE}$, $\overline{G}_{CTX}$ and $\overline{G}_{CTX}/G_F$ values obtained from specimens in a tube of the TS and FS samples are plotted against the depths in Fig. 23. The plots of G_{CTX} for the FS sample are located close to the curve for the depth of G_F

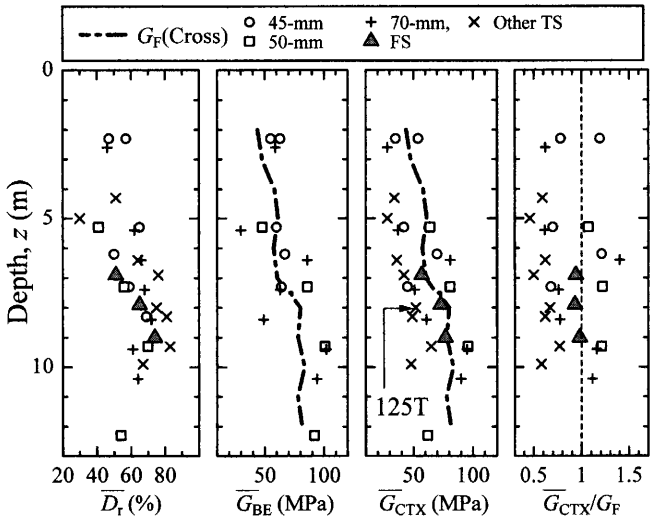

Fig. 23. The $\overline{D}_r$, $\overline{G}_{BE}$, $\overline{G}_{CTX}$ and $\overline{G}_{CTX}/G_F$ values against the depths

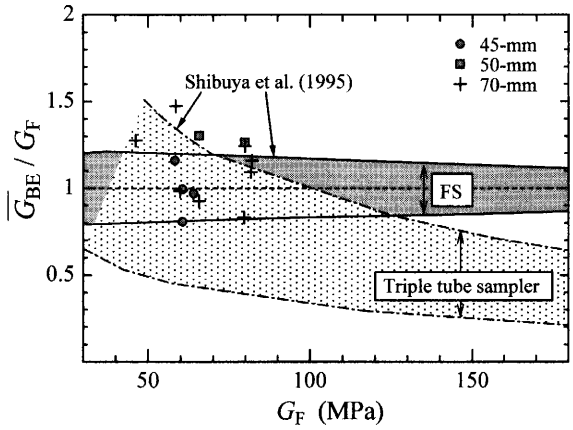

Fig. 24. Relationships between $\overline{G}_{BE}/G_F$ and G_F

and the $\overline{G}_{CTX}/G_F$ of the FS sample are almost 1.0. On the other hand, the $\overline{G}_{CTX}/G_F$ values obtained from the 45-mm, 50-mm and 70-mm samplers are in the range of 0.6 to 1.4 and greater than those of other TS samples (×). However, the $\overline{G}_{CTX}/G_F$ of other TS samples are in the range of 0.45 to 0.75 and the ratios are (25 ~ 55)% of the G_F from the FS, regardless of small $\overline{D}_r$ values. These coincide with the results of the R_{L20} in Figs. 15 and 19.

Figures 24 and 25 show the relationships between the ratios of $\overline{G}_{BE}/G_F$, $\overline{G}_{CTX}/G_F$ and G_F. The relationships between the initial modulus of rigidity and G_F by Shibuya et al. (1995) are also shown in these figures. From these figures, the results are summarized as follows:

1) The $\overline{G}_{BE}/G_F$ values from the 45-mm and 50-mm samplers are in the range of 0.8 to 1.3 and those plots are located inside and in the upper part of the area of the FS sample as shown by Shibuya et al. (1995). Therefore, the 45-mm and 50-mm samplers can take equally high quality samples as the FS sample, concerning the G_{BE}, in the range of $G_F = 46 \sim 82$ MPa, as in Niigata sands.
2) The $\overline{G}_{CTX}/G_F$ values from the 45-mm and 50-mm

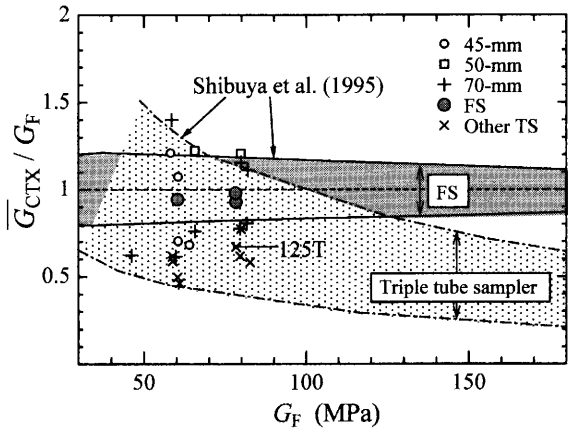

Fig. 25. Relationships between $\overline{G}_{CTX}/G_F$ and G_F

samplers are in the range of 0.7 to 1.2 and within those of the triple tube sampler. It means that the sample quality obtained from the 45-mm and 50-mm samplers is similar to those of the triple tube sampler commonly used in Japan. However, the $\overline{G}_{CTX}/G_F$ values from the triple tube sampler used in Niigata sand are smaller than those of the 45-mm and 50-mm. This has the same effect on the R_{L20} as shown in Fig. 16.

CONCLUSIONS

The conclusions obtained in this study are summarized as follows:

1) The relationship between the relative density (D_r) and normalized SPT N-value (N_1) obtained from small diameter samplers with inner diameters of 45 mm and 50 mm samplers was close to that of the frozen sample (FS) and the N_1 coefficient was greater than those of the 70-mm and other tube samplers.
2) The stress ratio at 20 cycles (R_{L20}) and initial modulus of rigidity (G_{CTX}) of samples obtained from the 45-mm and 50-mm samplers were greater than those of the 70-mm, 125-mm rotary triple-tube and other tube samplers. However, the R_{L20} values obtained from the 45-mm and 50-mm samplers were smaller than those of the FS sampler in the area of $N_1 > 24$.
3) The R_{L20} values estimated from Suzuki et al. (1995) could adequately describe the measured values, except for the plots of $z \fallingdotseq 25$ m. The Robertson et al. (1992) method adequately described those of the FS sample for depths exceeding 8 m.
4) The G_{BE} and G_{CTX} values obtained from the 45-mm and 50-mm samplers were close to those of the FS sampling, in the range of $G_F = 46 \sim 82$ MPa, as in Niigata sands.

ACKNOWLEDGEMENTS

The authors wish to express their sincere gratitude to the members of the Board of Education of the Niigata city government and the Meike elementary school for their cooperation in the sampling investigation and also to Vice-president Kakuichirou Adachi of the Shibaura Institute of Technology and President Yorio Makihara of Arufa Geo. Co., LTD. for information on the JGS-1989 investigation. Also to Dr. Akihiko Uchida (Takenaka Koumuten Co., Ltd.) and Ms Takeko Mikami (Oyo Corporation., Ltd.) in the bender element and cyclic triaxial tests and their interpretation.

NOTES

*The 45-mm sampler has two inner changeable tubes, one with a 45 mm inner diameter and the other with a 48 mm inner diameter.

NOTATION

BE: bender element test
CTX: cyclic triaxial test
F_c: percentage of grain size smaller than 0.075 mm
D_r: relative density
G_{BE}: initial modulus of rigidity from bender element test
G_{CTX}: initial modulus of rigidity from cyclic triaxial test
R_{L20}: liquefaction strength under $N_c = 20$
R_r: sample recovery ratio
N: number of blows of the Standard Penetration Test (SPT)
N_c: number of loading cycles
q_c: cone index of the Cone Penetration Test (CPT)
q_t: modified tip resistance of the cone on the q_c value for water pressure
q_{t1}: eliminated value for the σ'_{vo} from q_t
V_s: secondary wave velocity
σ_d: cyclic deviation stress
σ'_c: effective confined pressure
σ'_{vo}: effective overburden pressure
Δu: excess water pressure

REFERENCES

1) Ishihara, K. (1985): Stability of natural deposits during earthquakes, *Proc. 11th ICSMGE*, **1**, 321–390.
2) Japan Geotechnical Consultant Association (1998): Collaborative study on liquefaction of soils technical forum 1998, 341.
3) Japanese Geotechnical Society (1988): A report on the sampling and evaluating sample quality methods for sand deposits, the Soil Sampling-Committee of the Japanese Society for Soil Mechanics and Geotechnical Engineering, 71 (in Japanese).
4) Japanese Geotechnical Society (2000a): Preparation of soil specimens for triaxial tests (JGS 0520-2000), *Japanese Standards for Laboratory Soil Test Methods—Standards and Explanations—*, 443–448 (in Japanese).
5) Japanese Geotechnical Society (2000b): Methods for cyclic undrained triaxial test on soils (JGS 0541-2000), *Japanese Standards for Laboratory Soil Test Methods—Standards and Explanations—*, 642–678 (in Japanese).
6) Japanese Geotechnical Society (2000c): Method for cyclic triaxial test to determine deformation properties of geomaterials (JGS 0542-2000), *Japanese Standards for Laboratory Soil Test Methods—Standards and Explanations—*, 659–678 (in Japanese).
7) Japanese Geotechnical Society (2004a): Method for obtaining soil samples using thin-walled tube sampler with fixed piston (JGS 1221-2003), *Standard of Japanese Geotechnical Society for Soil Sampling-Standards and Explanations—*, 1–7.
8) Japanese Geotechnical Society (2004b): Method for obtaining soil samples using rotary double-tube sampler (JGS 1222-2003), *Standard of Japanese Geotechnical Society for Soil Sampling—Standards and Explanations—*, 8–11.

9) Japanese Geotechnical Society (2004c): Method for electric cone penetration test (JGS 1435-2003), *Japanese Standards for Geotechnical and Geoenvironmental Investigation Methods—Standards and Explanations—*, 301–309 (in Japanese).
10) Japanese Geotechnical Society (2004d): *Japanese Standards for Geotechnical and Geoenvironmental Investigation Methods—Standards and Explanations—*, 183 (in Japanese).
11) Japan Public Highway Corporation (2003): *Specifications for Highway Bridges* (in Japanese).
12) Meyerhof, G. G. (1957): Discussion for Session 1, *Proc. 4th ICSMFE*, London, **3**, 110.
13) Robertson, P. K., Woeller, D. J. and Finn, W. D. L. (1992): Seismic cone penetration test for evaluating liquefaction potential under cyclic loading, *Can. Geotech. J.*, **29**, 285–295.
14) Seed, H. B., Idriss, I. M. and Arango, I. (1983): Evaluation of liquefaction potential using field performance data, *J. Geotech. Engrg.*, ASCE, **109**(3), 458–482.
15) Shibuya, S., Mitachi, T., Yamashita, S., Tanaka, T., Nakajima, M., Furukawa, S. and Inahara, H. (1995): Measurement of small strain shear modulus of natural ground—effects of sampling methods—, *Proc. Symp. Sampling*, 71–78 (in Japanese).
16) Shogaki, T. (1997): A small diameter sampler with a two-chambered hydraulic piston and the quality of its samples, *Proc. 14th ICSMFE*, Hamburg, 201–204.
17) Shogaki, T. and Sakamoto, R. (2004): The applicability of a small diameter sampler with a two-chambered hydraulic piston for Japanese clay deposits, *Soils and Foundations*, **44**(1), 113–124.
18) Shogaki, T., Nakano, Y. and Shibata, A. (2002): Sample recovery ratios and sampler penetration resistance in tube sampling for Niigata sand, *Soils and Foundations*, **42**(5), 111–120.
19) Suzuki, Y., Tokimatsu, K., Taya, Y. and Kubota, Y. (1995): Relationship between CPT data, SPT data and liquefaction resistance of in-situ frozen samples, *Proc. 31st Ann. Conf. JGS*, 983–984 (in Japanese).
20) Tatsuoka, F., Yasuda, S., Iwasaki, T. and Tokida, K. (1980): Normalized dynamic undrained strength of sands subjected to cyclic and random loading, *Soils and Foundations*, **20**(3), 1–14.
21) Tokimatsu, K. and Ohhara, A. (1990): Frozen sampling, *Tsuchi-To-Kiso*, **38**(11), 61–68 (in Japanese).
22) Tokimatsu, K. and Uchida, A. (1990): Correlation between liquefaction resistance and shear wave velocity, *Soils and Foundations*, **30**(2), 33–42.
23) Tokimatsu, K. and Yoshimi, Y. (1983): Empirical correlation of soil liquefaction based on SPT *N*-value and fines content, *Soils and Foundations*, **23**(4), 56–74.
24) Uchida, A. (2003): A study on the evaluation of the cyclic deformation characteristics of sandy and gravel soils, *Doctorate Thesis*, Tokyo Institute of Technology (in Japanese).
25) Yoshimi, Y. (1994): Relationship among liquefaction resistance, SPT *N*-value and relative density for undisturbed samples of sands, *Tsuchi-To-Kiso*, **42**(4), 63–67 (in Japanese).
26) Yoshimi, Y., Tokimatsu, K. and Hosaka, Y. (1989): Evaluation of liquefaction resistance of clean sands based on high-quality undisturbed samples, *Soils and Foundations*, **29**(1), 93–104.